



# Thick Electrodes for High Energy Lithium Ion Batteries

Madhav Singh,<sup>a,z</sup> Jörg Kaiser,<sup>b</sup> and Horst Hahn<sup>a,c</sup>

<sup>a</sup>Institute of Nanotechnology, Karlsruhe Institute of Technology (KIT), 76344 Eggenstein-Leopoldshafen, Germany

<sup>b</sup>Project Competence-E, Karlsruhe Institute of Technology (KIT), 76344 Eggenstein-Leopoldshafen, Germany

<sup>c</sup>Helmholtz Institute Ulm for Electrochemical Energy Storage (HIU), 89081 Ulm, Germany

Thicker electrode layers for lithium ion cells have a favorable electrode to current collector ratio per stack volume and provide reduced cell manufacturing costs due to fewer cutting and stapling steps. The aim of this work is to investigate the delivery of energy in such cells compared to cells with thinner electrodes. In this regard, lithium ion cells with single sided 70  $\mu\text{m}$  and 320  $\mu\text{m}$  NMC based cathodes and graphite based anodes with low binder and carbon black contents were prepared and tested in half cell and full cell configurations. Thick and thin electrodes showed capacity losses of only 6% upon cycling at C-rates of C/10 and C/5 while cycling at C/2 resulted in significant losses of 37% for the thick electrodes and only 8% for the thin electrodes. Pouch cells with thick electrodes showed 19% higher volumetric energy density at C/5 in comparison to thinner electrodes. This can be an innovative approach to reduce cell costs and to achieve more competitive prices per energy for applications where only medium to small C-rates are required.

© The Author(s) 2015. Published by ECS. This is an open access article distributed under the terms of the Creative Commons Attribution 4.0 License (CC BY, <http://creativecommons.org/licenses/by/4.0/>), which permits unrestricted reuse of the work in any medium, provided the original work is properly cited. [DOI: 10.1149/2.0401507jes] All rights reserved.

Manuscript submitted January 13, 2015; revised manuscript received March 17, 2015. Published April 1, 2015.

Lithium ion cells have undergone a remarkable development regarding energy density, power density, lifetime, safety and costs since their market introduction in the early 1990s. While the early applications focused mainly on consumer electronics, in the second half of the last decade electromobile and stationary energy storage applications moved into scope. Today the industry focuses strongly on cost targets in terms of dollars per Watthour, by lowering both material and production costs and increasing the energy density of the cells while maintaining other factors such as safety and lifetime constant on a high level.

Three different cell designs are usually considered for electromobile or stationary energy applications: (i) cylindrical cells, (ii) prismatic shaped cells in hard cases made from metal or plastics, and (iii) pouch bag or coffee bag cells. The latter are widely used and are typically 7 to 13 mm thick which correlates with a few dozen layers of anode and cathode sheets, depending whether they are designed to serve energy or power optimized purposes. To produce such a stack, electrodes need to be cut from an electrode roll for example via laser cutting or punching, cleaned from loose particles, picked up automatically and then placed alternately with high accuracy on top of the growing stack. Compared to other steps in cell production like tab welding, pouch foil packaging and sealing or electrolyte filling, this stapling process takes up a considerable amount of the total cell assembly time. With the goal of reducing the stack assembly time and increasing the throughput of the cutting and stacking machine we have considered to investigate the preparation and characterization of electrodes that are substantially thicker than conventional ones and which would decrease the number of sheets for an electrode stack of given capacity.

However, with increasing electrode thickness the mass transport limitations of lithium ions in the electrolyte phase as well as the impedance for electrons in the solid phase of the electrode become dominating. This will reduce the capacity of the cell due to higher overpotentials upon charging and discharging within fixed voltage limits. At the same time, the geometric current density in the separator is higher at a given C-rate for thick electrodes compared to thin ones which causes additional overpotential and, in case of charging, could lead to lithium plating on graphite particles in vicinity to the separator.

The concept of thick electrodes has been employed previously<sup>1,2,3</sup> where such electrodes have been fabricated on different substrates (e.g. metal foams, textiles and foils) without optimization of the calendaring process and with addition of a large amount of binder (~ 10 – 12 wt%). A ballmilling as well as a high temperature sintering approach has also been reported to prepare binder-free thick electrode pellets.<sup>4</sup>

However, these approaches are very different from the currently employed process technology for slurry and electrode production for stapled pouch bag cells.

In this work, we present a pair of an energy optimized anode and cathode based on synthetic graphite and NMC (111) as active materials – an active material combination that is commonly used in lithium ion cells for automotive or stationary applications. Two batches of single-sided electrodes of different thicknesses were prepared and characterized: the first one having 70  $\mu\text{m}$  thickness and the second one 320  $\mu\text{m}$  (excluding the thickness of current collector). Usually, the conventional high energy cells have electrodes in the order of ~ 50 - 60  $\mu\text{m}$  thickness. Therefore in this article, 70  $\mu\text{m}$  thick electrodes are considered as conventional lithium ion cell electrodes.

## Experimental

**Electrodes preparation.**— Commercially available battery grade cathode material  $\text{LiNi}_{1/3}\text{Mn}_{1/3}\text{Co}_{1/3}\text{O}_2$  (NMC, BASF, Germany) and anode material graphite SMG-A (Hitachi, Japan) were used as active materials. Solef 5130 PVDF (Solvay, Italy) was used as a binder, while Super C65 carbon black and KS6L graphite (Imerys, Switzerland, formerly Timal) were used as conductive agents. All materials and substrates were used as delivered. PVDF was dissolved in N-methylpyrrolidone (NMP) at 60°C under stirring.

The cathode slurry was prepared by mixing NMC (90 wt%), Super C65 carbon black (3 wt%), KS6L graphite (4 wt%) and PVDF (3 wt%), dissolved in NMP. The anode slurry was prepared by mixing graphite (90 wt%), Super C65 carbon black (5 wt%) and PVDF (5 wt%), dissolved in NMP. These mixtures were further stirred and homogenized with a dispersing system (Dissolver Dispermat CA40, VMA-Getzmann GmbH, Germany) for approximately 2 h. Finally, the slurries were deaerated under vacuum for 1 h to remove the bubbles. The cathode slurry was then casted on aluminum foil (thickness: 20  $\mu\text{m}$ ) and anode slurry was casted on copper foil (thickness: 10  $\mu\text{m}$ ). Anodes and cathodes of different thicknesses were prepared by varying the doctor blade height. The coated electrodes were dried in an oven at 120 °C in ambient atmosphere for 30 min.

A calendaring roll pressure was applied to reduce 10% on cathode side and 15% on anode side of the original thickness of the dried slurry film so that porosity could be maintained at 40% in cathodes and 45% in anodes. These values are somewhat higher than the ca. 30% porosity typically found in commercial electrodes. However, to minimize lithium ion transport losses in the electrolyte phase rather than improve electric conductivity and volumetric energy density of the layer, we opted for higher porosities.

<sup>z</sup>E-mail: [madhav.singh@kit.edu](mailto:madhav.singh@kit.edu)

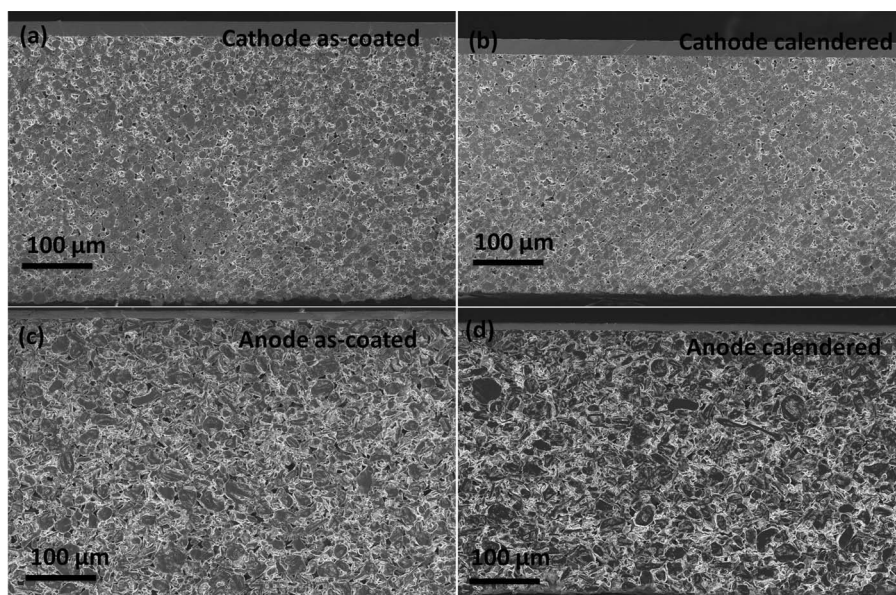


**Figure 1.** SEM images of cross-section of the (a) as coated NMC cathode, (b) calendered NMC cathode, (c) as coated graphite anode and (d) calendered graphite anode electrodes.

The average mass loadings of cathode and anode electrodes with 70  $\mu\text{m}$  and 320  $\mu\text{m}$  thicknesses (exclusive of current collector foil) were  $\sim 17 \text{ mg/cm}^2$  and  $\sim 72 \text{ mg/cm}^2$  and  $\sim 10 \text{ mg/cm}^2$  and  $\sim 43 \text{ mg/cm}^2$ , respectively. As far as we are concerned, there is no theoretical and experimental data available on such thick electrodes for a lithium ion cell.

Such thick electrodes are not suited for cylindrical or prismatic hard case cell formats where small winding radii in the order of 1 mm are applied in the center of the jelly roll. This would obviously form cracks and delaminate the active mass layer from the copper or aluminum substrates. However, we tested and wound the electrodes on roll cores with 3" inner diameter which are a standard in industrial electrode fabrication with electrode rolls of 1000 m and more length. We did not observe cracks or delamination proving sufficient flexibility and adhesion. With respect to the cell format, these electrodes are best suited for stacked cells with multiple anode and cathode sheets which is the preferred design for large format pouch cells.

**Cell preparation and characterization.**— For Swagelok cells the cathode and anode electrodes were punched into disks of 11 mm diameter and dried at 130°C under vacuum overnight. The cathode and anode disks were assembled in a two-electrode configuration against lithium metal foil as a counter electrode. A microporous glass fiber filter (Whatman) soaked in electrolyte was used as a separator. These half-cells were assembled in an argon filled glove box.

In addition, pouch bag cells with one anode and cathode sheet each were assembled in a dry room with dew points below  $-70^\circ\text{C}$ . The active areas of the cathodes and anodes sheets were  $5 \times 5 \text{ cm}^2$  and  $5.4 \times 5.4 \text{ cm}^2$ , respectively. It should be noted that during cutting and drying, both electrodes, Swagelok as well as pouch cell type, showed good mechanical integrity and stable edges. Electrodes were dried at 130°C under vacuum for overnight. Nickel and aluminum cell terminals were welded on anode and cathode electrodes by ultrasound, respectively. The electrolyte used in all cases was LP30 with Vinylencarbonate (11.5 wt%  $\text{LiPF}_6$ , 42.8 wt% EC, 42.8 wt% DMC, 2.9 wt% VC, BASF, Germany).

The cathode half-cells and lithium ion full cells were cycled galvanostatically at various currents in the voltage range of 3.0–4.2 V and potentiostatically at 4.2 V for 30 min using an Arbin BT 2000 battery tester and a Binder temperature chamber at constant 23°C. The anode half-cells were also cycled galvanostatically at various current rates in the voltage range of 2.0 V – 5 mV and potentiostatically at 5 mV for 30 min using the same setup and temperature. Scanning electron microscopy (Leo 1530 microscope) was used to view the

effect of calendaring pressure on the electrodes. Leica EM TIC 3X argon ion cutter was used to cut the cross- sections of the electrodes.

## Results and Discussion

**Scanning electron microscopy.**— Figure 1 shows the cross-section images of both as-coated and calendered cathode and anode electrodes. A significant difference is visible between the as-coated and calendered electrodes in the SEM images. The SEM images 1c and 1d clearly show that the pores shrink in size and electrodes are well compacted after calendaring in comparison to the as-coated electrodes. Furthermore, both pressed electrodes show evenly distributed active material particles and the pores in the cross-sections.

The SEM images of as-coated electrodes show a uniform, crack-free and stable coating throughout the electrode surface even with the low binder contents of only 3 wt% and 5 wt% that were used here for cathodes and anodes, respectively (Figure 2). Usually binder concentrations reported in the literature are higher but it was pointed out by Marks et al.<sup>5</sup> that commercial electrodes are optimized for high active material and low conducting aid and binder contents to maximize energetic densities. The authors evaluated that binder concentrations can vary from 4 to 12 wt% in the publications from the research community, which itself is a factor of two to six more than the 2 wt% of binder mentioned in one of the commercial electrodes (based on table 1 in Ref. 5). Low binder contents decrease the adhesion and mechanical stability with regard to electrode winding and cutting during cell assembly particularly in industrial production environments. Insufficient mechanical stability could result in loss of single particles or agglomerates of particles during the electrode cutting process which again could lead to shorts in case they are not properly removed and get stuck between anode and cathode and penetrate the separator, possibly leading to major malfunction of the cell. In our case the adhesion was strong and the edges of the electrode disks and square sheets showed good integrity.

High magnification SEM images (Figure 3) of calendered electrodes show no damaging of soft graphite and no change in the porosity of NMC spherical particles after the roll pressing. Besides the inter-particle pores available in the electrode layer, the NMC particles are made up by small primary crystallites with little, presumably 10 nm to 100 nm sized pores which probably also provide electrochemically active surface area. The coral like carbon black agglomerates are in both cases, anode and cathode, evenly dispersed over the surface of the active material particles and form a network which percolates to the substrate foil and provides good electric connectivity. Therefore, it is worth mentioning here that this ionic and electronic conductive



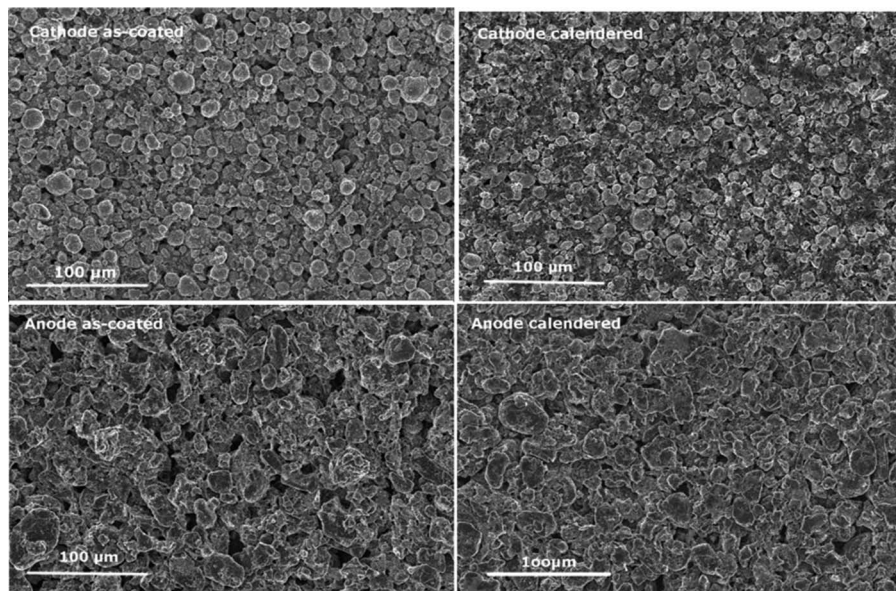


**Figure 2.** SEM images of surface of the (a) as coated NMC cathode, (b) calendered NMC cathode, (c) as coated graphite anode and (d) calendered graphite anode electrodes.

network, which is interconnected by particle to particle contacts, can provide a continuous ionic and electronic paths within the electrode layer from the substrate to the surface.<sup>6</sup>

**Half cell measurements.**— Next, the electrochemical behavior of thin and thick NMC cathodes during charging and discharging is investigated in a two-electrode, half cell Swagelok configuration versus lithium metal. It is followed by the analogous experiment with a graphite electrode.

**Cathodes.**— Figures 4a and 4b show the charge and discharge curves of 70  $\mu\text{m}$  and 320  $\mu\text{m}$  thick cathodes at different C-rates in the voltage range of 3–4.2 V where 1 C equals to 155 mA/g. Cathode half-cells exhibited discharge capacities of 142 mAh/g (100%) at 70  $\mu\text{m}$  thickness and 137 mAh/g (100%) at 320  $\mu\text{m}$  thickness at C/10 rate, of 138 mAh/g (97%) and 132 mAh/g (96%) at C/5 rate, and of 131 mAh/g (92%) and 86 mAh/g (63%) at C/2 rate, respectively. The discharge capacity values are quite satisfactory up to C/5 but as expected for thick electrodes, the discharge capacity deteriorated significantly at higher C-rates.

As already mentioned in the introduction two aspects should be considered here which are (i) longer diffusion and migration paths for lithium ions to enter or leave an electrode and (ii) higher local ion-current densities at the electrode/seperator interface. The first aspect contributes ohmic and mass transport losses to the overpotential in the electrode especially toward longer times of current flow, when kinetically favored particles in the upper region of the electrode have intercalated more lithium than the underlying regions and the remaining incoming ions need to migrate longer distances to the deeper lying regions in the electrode. This effect is more pronounced for the thick electrode where the overall current density at the electrode/seperator interface is 4.2 times as high as for the thin electrode (derived from the ratio of coating weight loadings in Electrodes preparation section). It is no surprise then, that the capacity of the 70  $\mu\text{m}$  thin electrode at C/2 with 131 mAh/g falls in the range of the capacity of the 320  $\mu\text{m}$  thick electrode at C/10 with 137 mAh/g. To account for this poorer lithium ion flux in the electrolyte filled pores of the electrodes with increasing electrode thickness we applied less calender force than usual for lithium ion electrodes as already mentioned in Electrodes preparation section.

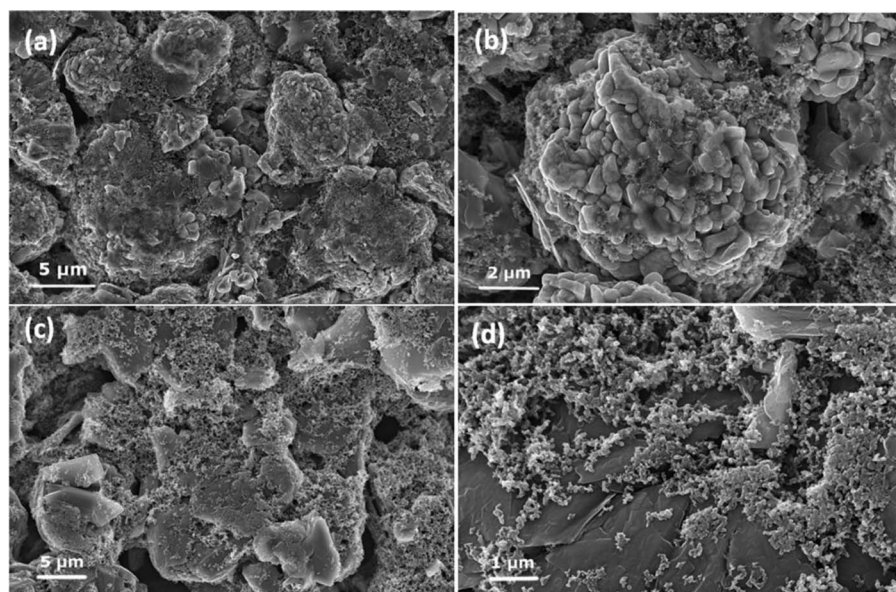


**Figure 3.** Higher magnified SEM images of calendered NMC cathode (a,b) and graphite anode (c,d) electrodes.

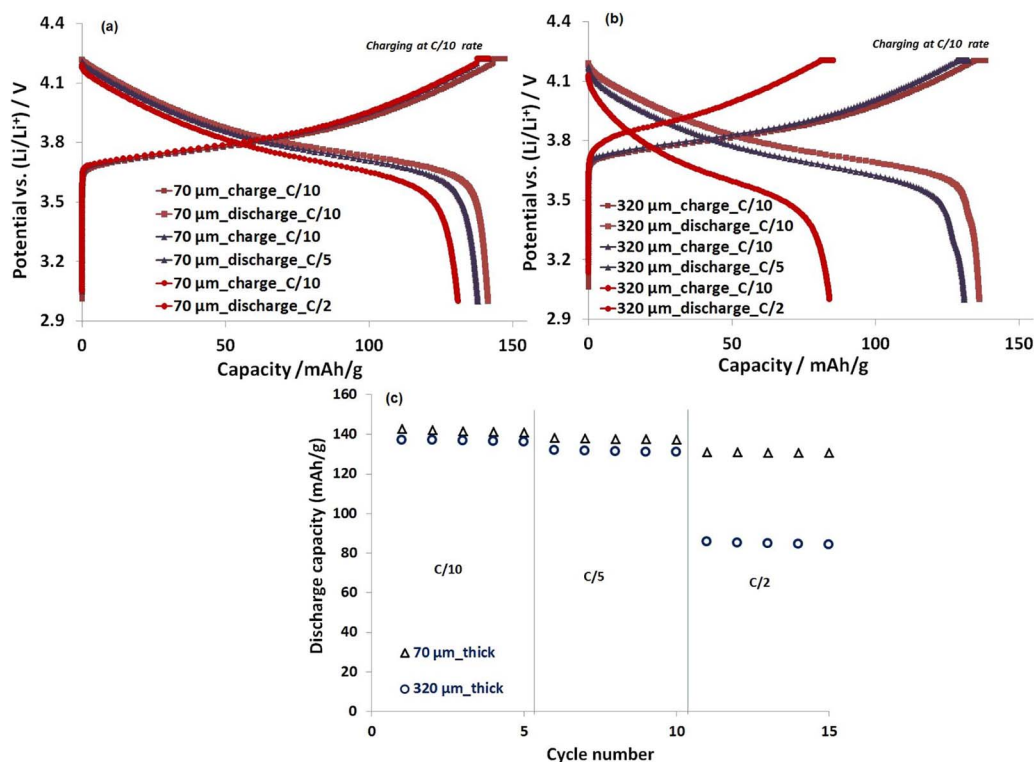


**Figure 4.** Cathode: Charge-discharge profiles (a,b) and comparison of rate capabilities (c) recorded at different C-rates of cathode half-cells (Swagelok type) with the 70  $\mu\text{m}$  and 320  $\mu\text{m}$  thick electrodes.

The second aspect are ohmic losses across the separator. In our case, the current density at the electrode/separator interface for a given C-rate is 4.2 times higher for the 320  $\mu\text{m}$  electrode in comparison to the 70  $\mu\text{m}$  electrode. This gives about  $4.2^2 \approx 18$  times the heat dissipation in the electrolyte ( $P_{\text{Loss}} = R \cdot I^2$ ) which would locally improve the mobility of ions and hence the ionic conductivity of the electrolyte thereby counteracting some of the ohmic limitations. While this aspect has probably no implications for the Swagelok type cells studied here with their high weight ratio of cell housing to active electrode and electrolyte mass, it might be of significance for large format pouch cells of several Ah in size, where heat is not that easily dissipated.

When discharged and charged repeatedly (Fig. 4c), thin and thick cathodes show reasonable stable capacities over the course of 5 cycles at each C rate. We would like to remind, that these cathodes have a PVDF binder content of only 3% and a carbon and graphite content of 7% in sum. With capacity losses between C/10 and C/2 discharge being 37% for the thick electrode and only 8% for the thin one, one has to consider that the energetic losses are even higher since the cell voltages have not yet been considered. This will be addressed in the Full cell measurements section where full cells were assembled and ran more cycles.

**Anodes.**—Figures 5a and 5b show the charge and discharge curves of the 70  $\mu\text{m}$  and 320  $\mu\text{m}$  thick anodes at different C-rates in the voltage range of 0.005–2 V where 1C is equal to 376 mA/g. Anode half-cells exhibited discharge capacities of 332 mAh/g (100%) at 70  $\mu\text{m}$  thickness and 262 mAh/g (100%) at 320  $\mu\text{m}$  thickness at C/10 rate, of 324 mAh/g (98%) and 245 mAh/g (94%) at C/5 rate, and of 318 mAh/g (96%) and 189 mAh/g (72%) at C/2 rate, respectively. The first two cycles at C/20 were used to form the SEI on the anode and we attribute deviations of 340 mAh/g found here from the 360 mAh/g specified by Hitachi to irreversible formation losses related to our electrolyte composition.

For both anodes studied here the variances in capacity and voltage profile are smaller than for the cathodes in Fig. 4a and 4b. However, it can be seen in Figure 5c that the thick electrode did not run stable and showed capacity losses throughout the first 12 cycles and even ceased

to operate in cycle 13. As far as we are concerned, we did not find any published data on such thick graphite based anodes for lithium ion cells at all. Therefore, we assume three factors to explain this loss: (i) Even the mild C/10 charge rate on the thick electrode correlates to a C/2.4 ionic current rate in the liquid phase at the electrode/separator interface (current density factor of 4.2, see above), which alone is still not stressful, but (ii) is experienced for 10 hrs by the graphite particles at the separator interface while (iii) the lithium metal counter electrode possesses a huge surplus of lithium and will virtually never cease to deliver lithium ions to the upper regions of the electrode with only little kinetic losses even after many cycles. As a consequence lithium plating is likely to have occurred and led to rapid aging and cell failure. The fact that in the full cell configuration in Full cell measurements section the cell was able to make much more cycles supports this theory.

**Full cell measurements.**— To complete the electrochemical characterization, anodes were then directly tested versus cathodes in full cell configuration in a more realistic pouch cell setup using  $5 \times 5 \text{ cm}^2$  sized electrodes and a commercial 30  $\mu\text{m}$  thin separator. This configuration eliminates the drawbacks of half cell measurements in the form of a lithium metal foil counter electrode, a 200  $\mu\text{m}$  thick filter paper separator and also minimizes detrimental edge effects due to larger sized electrodes compared to 11 mm diameter electrode disks in the Swagelok configuration. In general voltage losses during cell charging and discharging in this kind of full cell can be better compared to commercial systems and allow more realistic prediction of energy densities.

Looking at the capacities obtained from half-cell measurements at C/10 for cathode and anode, the balancing factor was 1.18 for the thick pair of electrodes and 1.35 for the thin pair of electrodes respectively. However, from the electrode preparation point of view and based on the theoretical capacities of 155 mAh/g for NMC and 376 mAh/g for graphite, we had intended to ideally obtain a balancing factor of 1.4. This shows that the kinetic losses are significant at these thicknesses and not all of the graphite is usable. However, if we



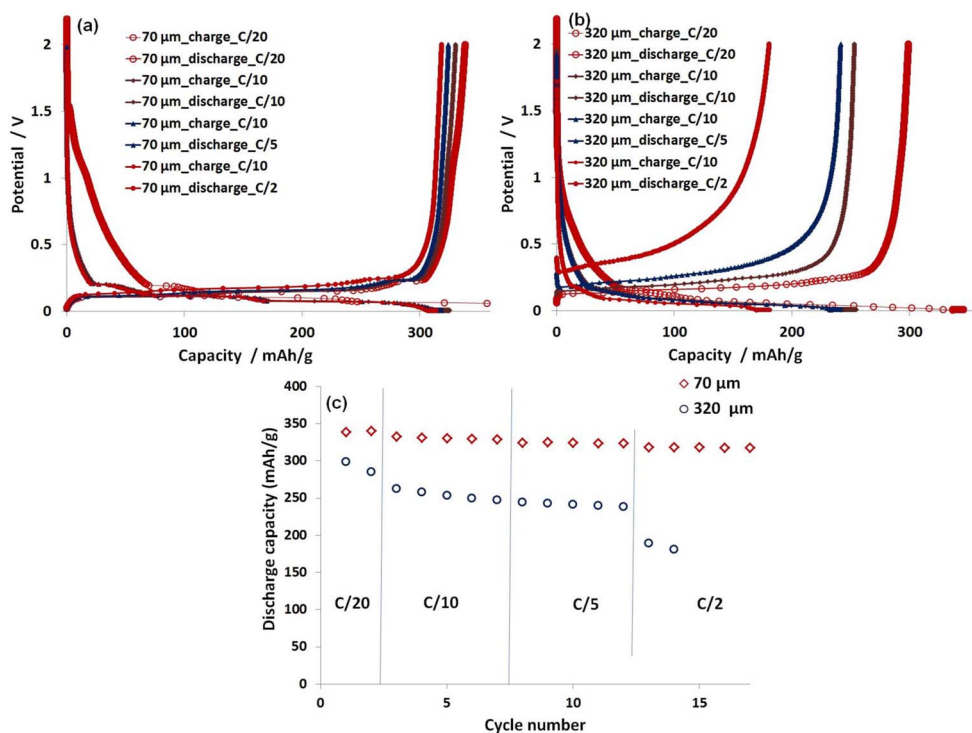


**Figure 5.** Anode: Charge-discharge profiles (a,b) and comparison of rate capabilities (c) recorded at different C-rates of anode half-cells (Swagelok type) with the 70  $\mu\text{m}$  and 320  $\mu\text{m}$  thick electrodes.

had chosen smaller anode loadings in the first place, we would have ended up with a balancing factor closer to 1 which would make over-saturation of graphite during charging and poorer cycle life stability more likely. On the other hand, balancing factors by far more than 1 are counter productive for the energy density of an anode/cathode pair.

Figures 6a and 6b show the galvanostatic charge-discharge profiles of 70  $\mu\text{m}$  and 320  $\mu\text{m}$  thick electrodes at different C-rates. Full cells delivered discharge capacities of 53 mAh (100%) at 70  $\mu\text{m}$  thickness and 233 mAh (100%) at 320  $\mu\text{m}$  thickness at C/10 rate, of 48 mAh (91%) and 221 mAh (95%) at C/5 rate, and of 45 mAh (85%) and 105 mAh (45%) at C/2 rate, respectively.

As expected from the half cell measurements the full cell with 320  $\mu\text{m}$  thick electrodes also shows significant capacity losses at C/2. However, to put these results into a quantitative context with commercial lithium ion cells, a simple calculation was done taking anode, cathode and separator and half of the substrate foils thicknesses into account (but excluded pouch foil and current tabs) to calculate the volume of an “unit cell” and its volumetric energy density in Wh/L. Figure 6c displays the resulting values for the measured cycles at C/10, C/5 and C/2.

An initial 337 Wh/L was found for the full cell with 70  $\mu\text{m}$  thickness. This value is in good agreement with values from commercial large format cells which show values in the order of 300 Wh/L to 350 Wh/L with LMO or NMC based cathodes.<sup>7,8</sup> On the one hand, the values from commercial cells are probably derived from the total cell volume including sealed edges and current tabs. On the other hand the anode / cathode balancing in our unit cell is likely to be higher and counter productive for energy density. An increase of energy density from 337 Wh/L to 412 Wh/L is obtained when the electrode thickness is increased from 70  $\mu\text{m}$  to 320  $\mu\text{m}$ . This is a significant increase by 19% although the thicker electrode pair shows higher kinetic limitations than thinner ones.

The charge/discharge cycling shows a similar capacity loss for both types of cells, which is also a promising result. We had expected that mechanical strains in the anode layer due to expansion and contraction while charging and discharging would have caused faster deterioration

in the case of the thick electrodes but this was not the case. After applying cycles at C/2 rates, the capacities returned from cycle number 60 on at C/10 and C/2 back to their initial values.

Therefore, it can be concluded that these thick electrodes can be used to improve the volumetric energy density of a lithium ion cell. For applications where lithium ion batteries are used to store energy from renewable sources and provide it to houses, C-rates for both charging and discharging are in the order of C/10 to C/3 and do not see fast pulses or fast continuous charging like in electromobile applications. With this in mind, the kinetic limitations that are observed in our case at currents faster than C/5 our results are already promising.

### Implications on Cell Manufacturing

Our goal was to develop an approach to reduce production cost for commercial large format lithium ion cells. Production of thick electrodes described in this work would save both raw material for current collectors as well as process time for stacking the electrodes and separator sheets. Even if the binder content would be increased significantly, we do not believe that electrodes of this thickness are suitable for 18650 or similar wound cells because the active layer would crack and delaminate from the metal foil given the small winding radii. The thicknesses of today’s electrodes produced in industry are, besides other factors in the coating and drying steps, determined from the roll cores of electrode coils where usually 3 inch inner diameter plus wall strength of the core define the minimum bending radius. If thicker electrodes tend to crack and delaminate larger cores would be an easy approach to address this issue, apart from developing alternative techniques for electrode production.

Furthermore shorter stacking times increase the throughput of industrialized automated cell production lines which would additionally (i) save investment costs for stacking machines on the one hand and (ii) would allow to decrease the dry room size with its investment costs and operation expenses.

### Summary

In this work, mechanically stable and crack-free single sided cathode and anode lithium ion cell electrodes with thicknesses of

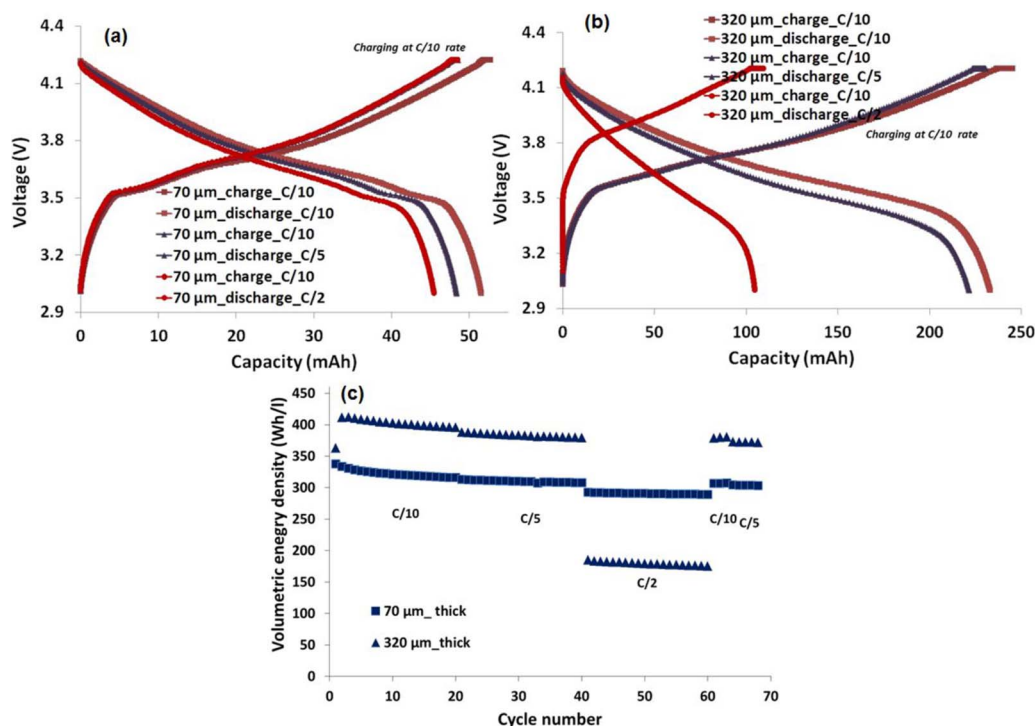


**Figure 6.** Full Cell: Voltage profile (a,b) and volumetric energy density (Wh/L) (c) graphs of lithium ion full cells (pouch cell) containing thin (70 μm) and thick electrodes (320 μm).

70 μm and 320 μm were prepared and tested in half cell and full cell configurations. Even with a low binder content in the laminate, the coatings were very stable, i.e. no delamination from the current collector foils, during the calendaring and preparation process. A slightly higher porosity ( $\geq 40\%$ ) was maintained in our thick electrodes in comparison to commercial electrodes so that a good ionic contact among the electrode particles as well as high lithium ion transport in the thick electrode can be obtained by the amount of electrolyte reserved in electrode pores. It was observed that at C-rates of C/2 significant capacity losses occur due to poor kinetics. Nevertheless, the thick electrodes approach could be sufficient for certain stationary energy storage applications where large batteries experience only small, continuous C-rates instead of fast pulse or fast continuous charging. In cases where applications require higher C-rates there is room for improvement by addressing the major aging mechanism which we believe is lithium plating during charging in the upper regions of the anode where the lithium ion flux in the electrolyte is highest.

#### Acknowledgment

Financial support by the German Ministry of Economics (BMWi) and the President of the Karlsruhe Institute of Technology (KIT)

is gratefully acknowledged. We also thank V. Wenzel, KIT, for his valuable support in slurry preparation.

#### References

1. J. S. Wang, P. Liu, E. Sherman, M. Verbrugge, and H. Tataria, "Formulation and characterization of ultra-thick electrodes for high energy lithium-ion batteries employing tailored metal foams," *J. Power Sources*, **196**, 8714 (2011).
2. L. Hu, F. L. Mantio, H. Wu, X. Xie, J. McDonough, M. Pasta, and Y. Cui, "Lithium-ion textile batteries with large areal mass loading," *Adv. Energy Mater.*, **1**, 1012 (2011).
3. H. Zheng, J. Li, X. Song, G. Liu, and V. S. Battaglia, "A comprehensive understanding of electrode thickness effects on the electrochemical performances of li-ion battery cathodes," *Electrochimica Acta*, **71**, 258 (2012).
4. W. Lai, C. Erdonmez, T. Marinis, C. Bjune, N. Dudney, F. Xu, R. Wartena, and Y. Chiang, "Ultrahigh-energy-density microbatteries enabled by new electrode architecture and micropackaging design," *Adv. Mater.*, **22**, E139 (2010).
5. T. Marks, S. Trussler, A. J. Smith, D. Xiong, and J. R. Dahn, "A guide to li-ion coin-cell electrode making for academic researchers," *J. Electrochem. Soc.*, **158**, A51 (2011).
6. J. Kaiser, V. Wenzel, H. Nirschl, B. Bitsch, N. Willenbacher, M. Baunach, M. Schmitt, S. Jaiser, P. Scharfer, and S. Schabel, "Prozess- und produktentwicklung von elektroden für li-ionen-zellen," *Chemie Ingenieur Technik*, **86**(5), 695 (2014).
7. XALT Energy, Data sheet for xalt 40ah high energy cell. <http://www.xaltenergy.com>.
8. Enertech. Data sheet for enertech international 40 ah high energy cell. (taken from homepage <http://www.enertechint.com>).